# Collision Rates in Charged Granular Gases

T. Scheffler and D.E. Wolf*
*Institut für Physik, Gerhard–Mercator–Universität Duisburg, D-47048 Duisburg, Germany*
(Dated: February 1, 2008)

The dissipation rate due to inelastic collisions between equally charged, insulating particles in a granular gas is calculated. It is equal to the known dissipation rate for uncharged granular media multiplied by a Boltzmann-like factor, that originates from Coulomb repulsion. Particle correlations lead to an effective potential that replaces the bare Coulomb potential in the Boltzmann factor. Collisional cooling in a granular gas proceeds with the known $t^{-2}$-law, until the kinetic energy of the grains becomes smaller than the Coulomb barrier. Then the granular temperature approaches a time dependence proportional to $1/\ln t$. If the particles have different charges of equal sign, the collision rate can always be lowered by redistributing the charge, until all particles carry the same charge. Finally granular flow through a vertical pipe is briefly discussed. All results are confirmed by computer simulations.

PACS numbers: PACS numbers: 45.70.-n, 05.20.Dd, 82.20.Pm

## I. INTRODUCTION

The particles in most granular materials carry a net electrical charge. This charge emerges naturally due to contact electrification during transport or is artificially induced in industrial processes. It is well known [1, 2, 3], for instance, that particles always get charged when transported through a pipe. In industry, contact electrification is used for dry separation of different plastic materials or salts [4], which tend to get oppositely charged and hence are deflected into opposite directions when falling through a condensor. Another application is powder varnishing, where uniformly charged pigment particles are blown towards the object to be painted, which is oppositely charged. Opposite charges are also used to cover one kind of particles with smaller particles of another kind in order to reduce van-der-Waals cohesion e.g. for inhalable drugs.

Whereas the dynamics of electrically neutral grains has been studied in great detail, little is known about what will change, if the grains are charged. In this paper we present the answer for collisional cooling, a basic phenomenon, which is responsible for many of the remarkable properties of dilute granular media. By collisional cooling one means that the relative motion of the grains, which lets them collide and can be compared to the thermal motion of molecules in a gas, becomes weaker with every collision, because energy is irreversibly transferred to the internal degrees of freedom of the grains.

In 1983 Haff [5] showed, that the rate, at which the kinetic energy of the relative motion of the grains is dissipated in a homogeneous granular gas, is proportional to $T^{3/2}$, where $T$ is the so called granular temperature. It is defined as the mean square fluctuation of the grain velocities divided by the space dimension:

$$T = \langle \vec{v}^{\,2} - \langle \vec{v} \rangle^2 \rangle / 3. \tag{1}$$

A consequence of this dissipation rate is that the granular temperature of a freely cooling granular gas decays with time as $t^{-2}$. We shall discuss, how these laws change, if the particles are uniformly charged.

Due to the irreversible particle interactions large scale patterns form in granular media, such as planetary rings [6] or the cellular patterns in vertically vibrated granular layers [7, 8, 9]. This happens even without external driving [10, 11, 13], where one can distinguish a kinetic, a shearing and a clustering regime. The regimes depend on the density, the system size and on the restitution coefficient $e_{\rm n} = -v'_{\rm n}/v_{\rm n}$, which is the ratio of the normal components of the relative velocities before and after a collision between two spherical grains. The $T^{3/2}$ cooling law holds, provided the restitution coefficient may be regarded as independent of $v_{\rm n}$ [19], and the system remains approximately homogeneous [12]. The latter condition defines the kinetic regime, which is observed for the highest values of the restitution coefficient, whereas the two other regimes are more complicated because of the inhomogeneities. Such inhomogeneities can only occur as transients, if all particles are equally charged, because the Coulomb repulsion will homogenize the system again.

*Electronic address: d.wolf@uni-duisburg.de

In order to avoid additional dissipation mechanisms due to eddy currents within the grains we consider only insulating materials. Unfortunately, up to now, no consistent microscopic theory for contact electrification of insulators exists [14]. In powder processing two types of charge distribution are observed [3]: A bipolar charging, where the charges of the particles in the powder can have opposite sign and the whole powder is almost neutral. The other case is monopolar charging, for which the particles tend to carry charges of the same sign and the countercharge is transferred to the container walls. It depends largely on the type of processing, whether one observes bipolar or monopolar charging, which means, that the material of the container, the material of the powder and other more ambiguous things, like air humidity or room temperature are important [14].

The outline of this article is as follows: The next section specifies the model we are considering. A simple derivation of the dissipation rate in dilute charged granular media based on kinetic gas theory is given in Sec. III. Sec. IV compares the analytic results with computer simulations. We find that in non-dilute systems the Coulomb repulsion is effectively reduced. This reduction will be explained, and we determine its dependence on the solid fraction of the granular gas. Then we apply these results to collisional cooling in Sec. V. Sec. VI addresses several aspects which are important for the applicability of the results for the dissipation rate: Are they valid locally in inhomogeneous systems, e.g. in the presence of container walls? What are the implications for granular flow through a vertical pipe? How does the dissipation rate change, if the particles carry different charges of equal sign? Finally, in Sec. VII we summarize our results. In appendix A we explain the simulation method we developed for this investigation [47].

## II. THE MODEL

In this paper, we consider monopolar charging, which is the usual case if insulators are transported through a metal pipe [2, 3]. For simplicity we assume, that all particles have the same point charge $q$ centred in a sphere of diameter $d$ and mass $m$. No polarization and no charge transfer during contact will be considered. The particle velocities are assumed to be much smaller than the velocity of light, so that relativistic effects (retardation and magnetic fields due to the particle motion) can be neglected. The electrodynamic interaction between the particles can then be approximated by the Coulomb potential:

$$\Phi_{ij} = q^2/r_{ij}, \tag{2}$$

where $r_{ij}$ is the distance between the centers of particles $i$ and $j$.

We consider the collisions as being instantaneous, which is a good approximation for the dilute granular gas, where the time between collisions is much longer than the duration of a contact between two particles. As the incomplete restitution ($e_\mathrm{n} < 1$) is the main dissipation mechanism in granular gases, Coulomb friction will be neglected in this paper. Also, the dependence of the restitution coefficient on the relative velocity [18, 19] will be ignored, so that the constant $e_\mathrm{n}$ is the only material parameter in our model.

The particles are confined to a volume $V = L^3$ with periodic boundary conditions in all three directions. The pressure in the system has two positive contributions, one kinetic and one due to the Coulomb repulsion. Although there are no confining walls, the system cannot expand because the periodic boundary conditions mean topologically, that the particles are restricted to a hypertorus of fixed volume. As we are going to show in Sec.VI A, the periodic volume can be thought of as a sufficiently homogeneous subpart of a larger system, which is kept from expanding by reflecting walls.

For vanishing particle diameter this model corresponds to the One Component Plasma (OCP) [15]. In the OCP a classical plasma is modelled by positive point charges (the ions) acting via the Coulomb potential, whereas the electrons are considered to be homogeneously smeared out over the whole system. In the OCP the electron background cannot be polarised, i.e. Debye screening does not exist, as is the case in our model, too.

In order to take the periodic images of the simulation cell into account we used an Ewald summation. It is only possible for the forces – which is all one needs in a molecular dynamics simulation.[49] We checked that for our simulation parameters only the nearest periodic images of a particle contribute noticably to the force, so that most of our data could be obtained with the simple minimum image convention instead of the Ewald summation.

## III. ANALYTICAL RESULTS FOR DILUTE SYSTEMS

In this section we derive an approximate expression for the dissipation rate in a dilute system of granular spheres, which interact with a purely repulsive, rotationally invariant pair potential. The reasoning is a simple adaptation of the kinetic theory of a hard sphere gas with inelastic collisions [22, 23]. In particular we assume that the pair potential is sufficiently well behaved that correlations of the particles are unimportant in the dilute limit, that the

particle density remains uniform and that the velocity distribution remains approximately Gaußian in spite of the nonstationarity due to the collisional cooling process.

It is one of the surprising results of the computer simulations presented in the next section that these assumptions give the correct high temperature behaviour even for the Coulomb interaction, which is known not to be "well behaved" in the above sense because of its long range [20]. One reason for the applicability is that the hard core repulsion sets an upper bound on the Coulomb interaction $\Phi_{ij} \leq q^2/d$. Hence, if the kinetic energy of the particles is much larger than this value, the collision rate will be approximately the same as in the uncharged case. This is a crucial simplification compared to charged point particles. Using the analytic form of the dissipation rate in the dilute limit derived here, we will discuss the dissipation in a non-dilute system, where correlations are important, in the next section.

We start with calculating the collision frequency of a fixed particle $i$ with any of the other particles $j$. If they were not charged, two particles would collide provided the relative velocity $\vec{u}$ points into the direction of the distance vector $\vec{r} = \vec{r}_j - \vec{r}_i$ connecting the particle centers, $\vec{u} \cdot \vec{r} > 0$, and the impact parameter $b = |\vec{r} \times \vec{u}|/u$ is smaller than the sum of the particle radii, $b \leq b_{\max} = d$. If the particles repel each other, the maximum impact parameter $b_{\max}$ becomes smaller than $d$. By the conservation laws for angular momentum and for energy one gets:

$$b_{\max}^2 = d^2 \left(1 - \frac{2E_{\mathrm{q}}}{\mu\, u^2}\right) , \tag{3}$$

where $\mu = m/2$ is the reduced mass. $E_{\mathrm{q}}$ denotes the energy barrier which must be overcome to let two particles collide in the dilute limit. It is the difference of the potential energies at contact and when they are infinitely far apart. Eq. (3) is independent of the actual form of the potential, as long as it has radial symmetry. (Note that energy is conserved as long as the particles do not touch each other.)

Imagine a beam of particles, all having the same asymptotic velocity $\vec{u}$ far away from particle $j$. All particles within an asymptotic cylinder of radius $b_{\max}$ around the axis through the center of $j$ with the direction of $\vec{u}$ will collide with particle $j$. There will be $\pi\, b_{\max}^2\, u\, n$ such collisions per unit time, where $n = N/V$ is the number density. Integrating over all relative velocities $\vec{u}$ gives the collision frequency of a single particle in the granular gas in mean field approximation:

$$f = \pi n \int\limits_{u \geq u_0} d^3u\, u\, b_{\max}^2(u)\, p(u) . \tag{4}$$

$u_0 = \sqrt{2E_{\mathrm{q}}/\mu}$ is the minimal relative velocity at infinity, for which a collision can occur overcoming the repulsive interaction. We assume that the particle velocity distribution is Gaußian with variance $3T$ (see (1)), so that the relative velocity will have a Gaußian distribution $p(u)$ as well, with

$$\langle u^2 \rangle = 6\, T . \tag{5}$$

Hence, the total number of binary collisions per unit time and per unit volume is given by:

$$\dot{N}_g = 1/2\, f\, n = 2\sqrt{\pi}\, n^2\, d^2\, \sqrt{T} \cdot \exp\left(-\frac{E_{\mathrm{q}}}{mT}\right) . \tag{6}$$

The factor $1/2$ avoids double counting of collisions. This corresponds to textbook physics for chemical reaction rates as can be found for example in Present[21].

Now we calculate the dissipation rate: The energy loss due to a single inelastic collision is:

$$\delta E(u, b) = \frac{\mu}{2} \left(1 - e_{\mathrm{n}}^2\right) u_{\mathrm{n}}^{*\,2} , \tag{7}$$

where $u_{\mathrm{n}}^*$ means the normal component of the relative velocity $\vec{u}^*$ at the collision. It can be calculated easily from $u_{\mathrm{n}}^{*2} = u^{*2} - u_{\mathrm{t}}^{*2}$: The tangential component is determined by angular momentum conservation,

$$\mu u b = \mu u_{\mathrm{t}}^* d , \tag{8}$$

and energy conservation gives

$$u^{*2} = u^2 \left(1 - \frac{2E_{\mathrm{q}}}{\mu\, u^2}\right) = u^2 \left(\frac{b_{\max}}{d}\right)^2 . \tag{9}$$

This yields

$$u_{\rm n}^{*\,2} = u^2 \frac{b_{\rm max}^2 - b^2}{d^2} \; . \tag{10}$$

The energy loss in one collision is therefore:

$$\delta E(u,b) = \frac{\mu}{2} \, \left(1 - e_{\rm n}^2\right) \, u^2 \, \frac{b_{\rm max}^2 - b^2}{d^2} \; . \tag{11}$$

Assuming a homogeneous distribution of particles, we eliminate the $b$-dependence by averaging over the area $\pi b_{\rm max}^2$:

$$\delta E(u) \;=\; \frac{1}{\pi b_{\rm max}^2} \int\limits_0^{b_{\rm max}} db \, 2\pi b \, \delta E(u,b) \tag{12}$$

$$\;=\; \frac{\mu}{4} \, u^2 \, \left(1 - e_{\rm n}^2\right) \left(1 - \frac{2E_{\rm q}}{\mu \, u^2}\right) \; . \tag{13}$$

The dissipated energy per unit time due to collisions with relative velocity $u$ is then the number of such collisions per unit volume, $1/2 \, n^2 \pi b_{\rm max}^2 \, u$, times the energy loss $\delta E$, Eq. (13).

Finally we get the dissipation rate per unit volume in the dilute limit ($\nu \to 0$) by integration over the relative velocity distribution:

$$\gamma \;=\; \frac{\pi}{2} n^2 \int\limits_{u \geq u_0} d^3u \, b_{\rm max}^2 \, u \, \delta E(u) \, p(u)$$

$$\;=\; 2\sqrt{\pi} \, n^2 d^2 m \, \left(1 - e_{\rm n}^2\right) \, T^{3/2} \cdot \exp\left(-\frac{E_{\rm q}}{mT}\right) \; . \tag{14}$$

The dissipation rate of an *uncharged* granular system in the dilute limit in the kinetic regime is given by [5]:

$$\gamma_0 = 2\sqrt{\pi} \, n^2 d^2 m \, \left(1 - e_{\rm n}^2\right) \, T^{3/2} \; . \tag{15}$$

Thus the dissipation rate (14) in a dilute granular gas with repulsive pair interactions and the one for the uncharged case differ only by a Boltzmann factor, $\gamma = \gamma_0 \cdot \exp\left(-E_{\rm q}/mT\right)$. This is the main result of the analytic treatment in this section.

If all grains carry the charge $q$, the potential barrier is $E_{\rm q} = q^2/d$. Our simulation results, Fig. 1, show that (14) is applicable in the dilute case at least for $E_{\rm q}/mT < 10$. For smaller granular temperature, however, we expect that corrections to (14) due to the long range of the Coulomb potential become important.

## IV. DISSIPATION RATE FOR DENSE SYSTEMS

In order to discuss the dissipation rate $\gamma$ in a non-dilute system of charged granular matter, let us recall the analytic form of $\gamma$ in an uncharged non-dilute system. The derivation is basically done by using the Enskog expansion of the velocity distribution function for dense gases [22]. One finds that (15) underestimates the collision rate (hence also the dissipation rate) because it does not take the excluded volume into account. The corrected dissipation rate for a non dilute uncharged system is:

$$\gamma = \gamma_0 \cdot g_{\rm hs}(\nu) \; , \tag{16}$$

where $\gamma_0$ is given by Eq. (15) and $g_{\rm hs}(\nu) > 1$ is the equilibrium pair distribution function of the non-dissipative hard-sphere fluid at contact. It only depends on the solid fraction $\nu = \pi n d^3/6$:

$$g_{\rm hs}(\nu) = \frac{2 - \nu}{2(1-\nu)^3} \tag{17}$$

(Carnahan and Starling [24], Jenkins and Richman [23]).

Our system consists of dissipative charged hard-spheres (CHS). The Boltzmann factor in Eq. (14) is just the equilibrium pair distribution function at contact in the dilute limit for a CHS-fluid, $\lim_{\nu\to 0} g_{\mathrm{chs}}(\nu, q) = \exp(-E_{\mathrm{q}}/mT)$. So it is plausible, that the dissipation rate for a dense system of dissipative CHS should be

$$\gamma = \gamma_0 \cdot g_{\mathrm{chs}}(\nu, q) \; . \tag{18}$$

Unfortunately the literature is lacking a satisfying analytic expression for $g_{\mathrm{chs}}$. In 1972 Palmer and Weeks [25] did a mean spherical model for the CHS and derived an analytic expression for $g_{\mathrm{chs}}$, but this approximation is poor for low densities. Many methods [26] give $g_{\mathrm{chs}}$ as a result of integral equations, that can be solved numerically. We do not use those approximations, but make the following ansatz for $g_{\mathrm{chs}}$:

$$g_{\mathrm{chs}}(\nu, q) \approx g_{\mathrm{hs}}(\nu) \cdot \exp\left(-\frac{E_{\mathrm{eff}}(\nu)}{mT}\right) \; . \tag{19}$$

As in the dilute case we assume that the long range Coulomb repulsion modifies the pair distribution function of the uncharged hard sphere gas by a Boltzmann factor. Note that the granular temperature enters the pair distribution function only through this Boltzmann factor. The hard core repulsion is not connected with any energy scale, so that the pair distribution function $g_{\mathrm{hs}}$ cannot depend on $T$. The effective energy barrier $E_{\mathrm{eff}}$ must approach $E_{\mathrm{q}} = q^2/d$ in the dilute limit. Hence the ansatz (19) contains both the uncharged and the dilute limit, (16) respectively (14).

In order to check the ansatz (19) we did computer simulations using the MD algorithm as described in the appendix [47]. Test systems of varying solid fraction $\nu$ and particle number ranging from $N = 256$ to $N = 1024$ were prepared at a starting temperature $T_0$. As soon as the simulation starts, the granular temperature drops because of the inelastic collisions. We measured the dissipation rate $\gamma$ and the granular temperature during this evolution. According to Eq. (19) and Eq. (18) the dissipation rate is $\gamma = \gamma_0\, g_{\mathrm{hs}}(\nu) \cdot \exp(E_{\mathrm{eff}}(\nu)/mT)$. An Arrhenius plot ($\ln(\gamma/\gamma_0\, g_{\mathrm{hs}})$ versus $E_{\mathrm{q}}/mT$) should give a straight line whose negative slope is the effective energy barrier $E_{\mathrm{eff}}$. Fig. 1 shows two examples of these simulations. The Arrhenius plots are linear to a very good approximation. This confirms the ansatz (19). Systems with high densities show slight deviations from linearity.

The negative slopes $E_{\mathrm{eff}}/E_{\mathrm{q}}$ in Fig. 1 are smaller than 1, which means, that the effective energy barrier is smaller than in the dilute system. The explanation is that two particles which are about to collide not only repel each other but are also pushed together by being repelled from all the other charged particles in the system.

For dimensional reasons the effective energy barrier to be overcome, when two particles collide, must be of the form

$$E_{\mathrm{eff}} = \frac{q^2}{d} - \frac{q^2}{\ell} f(d/\ell) \; , \tag{20}$$

where $\ell > d$ is the typical distance between the charged particles and $f$ is a dimensionless function. The first term is the Coulomb interaction $E_{\mathrm{q}}$ of the collision partners at contact. The second term takes the interaction with all other particles in the system into account. It is negative, because the energy barrier for the collision is reduced in dense systems.

Obviously, for a dense packing, $\ell \to d$, the energy barrier for a collision must vanish, i.e. $E_{\mathrm{eff}}|_{d=\ell} = 0$. Moreover, if one takes a dense packing and reduces the radii of all particles infinitesimally, keeping their centers in place, all particles should be force free for symmetry reasons. Therefore, the energy barrier must vanish at least quadratically in $(\ell - d)$, i.e. $\partial E_{\mathrm{eff}}/\partial d|_{d=\ell} = 0$. For the function $f$ this implies

$$f(1) = 1 \qquad \text{and} \qquad \left.\frac{\mathrm{d}f(x)}{\mathrm{d}x}\right|_{x=1} = -1. \tag{21}$$

If the particle diameter $d$ is much smaller than the typical distance $\ell$ between the particles, the function $f(d/\ell)$ may be expanded to linear order,

$$f(x) = c_0 + c_1 x + \ldots \tag{22}$$

In linear approximation the coefficients are determined by (21): $c_0 = 2$ and $c_1 = -1$. This determines the energy barrier (20).

In 1969 Salpeter and Van Horn [27, 33] pointed out, that inside a strongly coupled OCP a short-range body centered cubic (BCC) ordering will emerge. In the BCC lattice the nearest neighbour distance $\ell$ is related to the volume fraction $\nu$ by

$$\frac{d}{\ell} = \frac{2}{\sqrt{3}} \left(\frac{3}{\pi}\nu\right)^{1/3} \approx 1.14\, \nu^{1/3}. \tag{23}$$

Assuming a BCC structure and using the linear approximation for $f(x)$ in (20), the effective energy barrier is therefore given by

$$E_{\rm eff} = E_{\rm q}\left(1-\frac{d}{\ell}\right)^2 = E_{\rm q}\left(1-2.27\,\nu^{1/3}+1.29\,\nu^{2/3}\right) \tag{24}$$

To test Eq. (24) we simulated systems with densities ranging from $\nu = 0.001$ to $\nu = 0.216$ and determined the ratio $E_{\rm eff}(\nu)/E_{\rm q}$ as in Fig. 1. The results are plotted in Fig. 2. The agreement of the theoretical formula (24) with the simulations is excellent. One can see, that in the dilute limit the effective energy barrier extrapolates to $E_{\rm q}$. We cannot simulate systems with very low density, because collisions are too unlikely.

For the highest densities one cannot expect that the linear approximation (22) remains valid. Also, the dense packing of spheres is achieved with an FCC (face centered cubic) rather than a BCC ordering. This may be responsible for the systematic slight deviation from the theoretical curve in Fig. 2. A more refined analysis [48] of the pair distribution function leads to $d/\ell \approx 1.20\nu^{1/3}$ instead of (23). This fits the data for large $\nu$ in Fig.24 slightly better.

The reduction of the Coulomb repulsion was also found in the OCP, when it was applied to dense stars [27]. There the analogue of the second term in (20) is called the "screening potential" (somewhat misleadingly, as there is no polarizable counter charge and hence no screening). Monte Carlo simulations [29] of the OCP were interpreted in terms of a linear "screening potential" [28], which corresponds to (22), and the analogue of the conditions (21) also occurs in the plasma context [30], although based on a different physical reasoning. Corrections to the linear approximation are the subject of current research [31]. However, applying these more sophisticated forms of the "screening potential" of the OCP model to dense charged granular gases seems arguable as for higher densities the influence of the hard spheres become more and more important and so the analogy to the OCP model, which uses point charges, does no longer hold.

We showed that (18) and (19) also hold in two dimensions with [41, 42]

$$\gamma_0^{\rm 2D} = \sqrt{\pi}\,n^2 dm\,\left(1-e_{\rm n}^2\right)T^{3/2},$$

$$g_{\rm hs}^{\rm 2D}(\nu) = (1-\frac{7}{16}\nu)/(1-\nu)^2 \quad \text{and} \tag{25}$$

$$E_{\rm eff} = E_{\rm q}(1-d/\ell)^2 \quad \text{as in three dimensions.}$$

## V. TIME DEPENDENCE OF THE GRANULAR TEMPERATURE

The results for the dissipation rate suggest that one must distinguish two asymptotic regimes for collisional cooling in a charged granular gas: As long as the granular temperature of the granular gas is so high that the kinetic energy of the grains is much larger than the Coulomb barrier $E_{\rm eff}$, the charges can be neglected. The collisional cooling then proceeds initially like in the uncharged case, i.e. the granular temperature decreases as $t^{-2}$. However, as the kinetic energy approaches $E_{\rm eff}$ the charges become more and more important. Electrostatic repulsion suppresses the collisions, so that the collisional cooling slows down dramatically. This will be calculated in this section.

If one assumes that the dissipation of energy essentially changes only the kinetic energy, it follows that:

$$\frac{d}{dt}E_{\rm kin}/V = -\gamma\left(T(t)\right) \tag{26}$$

With $E_{\rm kin}/N = 1.5mT$ this gives a differential equation for $dT/dt$:

$$\frac{dT}{dt} = -\frac{2}{3}m^{-1}n^{-1}\gamma\left(T(t)\right) \tag{27}$$

This gives with (15), (18) and (19):

$$\frac{dT}{dt} = -\frac{4}{3}\sqrt{\pi}nd^2(1-e_{\rm n}^2)T^{3/2}\cdot g_{\rm hs}\cdot\exp\left(-\frac{E_{\rm eff}}{mT}\right) \tag{28}$$

As the total number of collisions is an increasing function in time, we can choose the number of collisions of particles, $c :=$ collisions$/N$, as a measure of time. This substitution is known from uncharged granular cooling [40]. We get

$$\frac{dT}{dc} = \frac{dT}{dt}/\frac{dc}{dt} = -\frac{2}{3}\left(1-e_{\rm n}^2\right)T(c) \tag{29}$$

where the derivative

$$\frac{dc}{dt} = 2\sqrt{\pi} n d^2 \sqrt{T} \cdot g_{\rm hs} \cdot \exp\left(-\frac{E_{\rm eff}}{mT}\right) \tag{30}$$

is derived from (6), (17) and (19). This gives the solution

$$T(c) = T_0 \cdot \exp\left(-\frac{2}{3}\left(1-e_{\rm n}^2\right) c\right) \tag{31}$$

where $T_0$ is the temperature, where the counting of collisions starts.

Fig. 3 shows the free cooling of a test system. The dashed line corresponds to the approximative solution of the theory given above, and the solid curve is the result of a computer simulation. The agreement between (31) and the simulation is very good. This means that the change of the overall potential energy can be neglected compared to the change of the kinetic energy for high temperatures.

An analytical solution of (28) is obtained by substituting

$$u = \sqrt{\frac{E_{\rm eff}}{mT}} \quad \text{and} \quad \tau = \left(\frac{2}{3}\sqrt{\pi} n d^2 (1-e_{\rm n}^2) g_{\rm hs} \sqrt{\frac{E_{\rm eff}}{m}}\right) t. \tag{32}$$

This gives

$$\frac{du}{d\tau} = \exp(-u^2) \tag{33}$$

with the initial condition $u(0) = \sqrt{E_{\rm eff}/mT_0}$. With the integral $I(u) = \int_0^u \exp(v^2) dv$, which is related to the probability function $\Phi(x) = (2/\sqrt{\pi}) \int_0^x \exp(-\xi^2) d\xi$ by

$$I(u) = \frac{\sqrt{\pi}}{2i} \Phi(iu), \tag{34}$$

the time $t(T, T_0)$ during which the granular temperature drops from $T_0$ to $T$ is given by

$$t(T, T_0) = \left(I\left(\sqrt{\frac{E_{\rm eff}}{mT}}\right) - I\left(\sqrt{\frac{E_{\rm eff}}{mT_0}}\right)\right) \Big/ C\sqrt{\frac{E_{\rm eff}}{m}} \tag{35}$$

with the constant

$$C = \frac{2}{3}\sqrt{\pi} n d^2 (1-e_{\rm n}^2) g_{\rm hs}. \tag{36}$$

For granular temperatures which are large compared to the Coulomb barrier, $T_0 > T \gg E_{\rm eff}/m$, the right hand side of (35) may be approximated as $I'(0)(T^{-1/2} - T_0^{-1/2})/C$. With $I'(0) = 1$ this reduces to the well known equation for the free cooling of an uncharged, homogeneous granular gas. For large initial granular temperature, $T_0 \to \infty$, one obtains a power law

$$T \approx (Ct)^{-2}. \tag{37}$$

This power law is only valid for $t \ll t_{\rm c} = (E_{\rm eff} C^2/m)^{-1/2}$. At $t_{\rm c}$, the granular temperature $T$ drops below $\sqrt{E_{\rm eff}/m}$. Then the repulsion between the charges on the particles becomes important. Using $I(u) \approx \exp(u^2)$ for large $u$ one obtains for $t \gg t_{\rm c}$

$$T \approx \frac{E_{\rm eff}}{m} \frac{1}{\ln(t/t_{\rm c})}. \tag{38}$$

## VI. A FEW APPLICATIONS TO HETEROGENEOUS SYSTEMS

### A. Influence of walls

Due to the long range of unscreened Coulomb interactions, monopolarly charged granular systems are always inhomogeneous in reality, because the influence of container walls is not restricted to their vicinity. Therefore it is

an important question, whether results obtained for homogeneous systems with periodic boundary conditions can be applied locally.

We checked this for a two dimensional charged granular gas confined in $x$-direction by walls, which are assumed to be uniformly charged and unpolarizable for simplicity so that their electrical field inside the box is zero. In $y$-direction periodic boundary conditions were imposed so that the system is translationally invariant in this direction.

The box was divided into equal layers parallel to the walls, and the properties were averaged over these layers. In this way the solid fraction shown in Fig.4 was obtained. As expected, the particle concentration increases towards the walls, because there is no Coulomb repulsion from particles outside the container. As screening is absent inside the box the solid fraction profile for fixed global solid fraction, $\nu = 0.186$ (averaged over the entire container), depends approximately only on the scaled variable $x/W$, where $W$ is the distance between the walls, with small deviations due to the excluded volume interaction.

Similarly we recorded the local granular temperature $T_{\rm loc}(x/W)$ (not shown) and the local dissipation rate, $\gamma_{\rm loc}(x/W)$. All these profiles depend on the global granular temperature, $T(t)$, which decreases due to collisional cooling. However, in order to get good statistics, we set the coefficient of restitution equal one in this simulation so that $E_{\rm q}/mT = 1.7$ remained constant. Hence the local profiles of the solid fraction and the granular temperature could be averaged over time. The local dissipation rate was calculated by taking for each collision the energy into account, which would have been dissipated if the coefficient of restitution had been zero.

Fig.5 shows the local dissipation rate in units of $\gamma_{\rm hom}$, the dissipation rate for a homogeneous system with the same global solid fraction and the same global temperature. It agrees very well with the theoretical prediction obtained from (18), (19) and (25), if one inserts the local solid fraction, $\nu_{\rm loc}$ (see Fig.4), and the local granular temperature, $T_{\rm loc}$. Apart from the immediate neighborhood of the wall the system is locally homogeneous enough that the results from the previous sections may be applied.

### B. Pipe flow

The flow of granular matter through a vertical pipe depends strongly on whether or not the particles are charged. First we recall the results for the uncharged case [43, 44]. Steady state flow is reached, when gravitational acceleration and friction at the walls balance each other. In this case, "friction" is due to collisions of grains with the wall, by means of which momentum is transfered and the particles are randomly scattered back. Hence the walls are permanent sources of granular temperature, which are balanced by the collisional cooling within the pipe. Fig. 6 shows typical steady state profiles of local volume fraction and local granular temperature across a pipe: The granular gas is dilute close to the walls, where the granular temperature is high, and gets compressed towards the middle of the pipe, where the granular temperature is low. For this inhomogeneity the pipe must not be too narrow.

Comparing this with Fig.4, it is obvious, that electrostatic repulsion counteracts the dilation near the wall and the compression in the interior of the pipe: If all particles carry charges of the same sign, the solid fraction profile will be flatter than in the uncharged case. The increased concentration near the walls will lead to more "friction" at the wall. Hence charged matter flows more slowly through a vertical pipe and may even get stuck for strong charging [45].

### C. Differently charged particles

In a real system the particles will carry different charges, even if they are equal in all other respects. The charging process may determine the sign of the charges, but the amount will in general fluctuate. Therefore it is important to discuss how the dissipation rate depends on the width of a charge distribution, if the total charge of the system is fixed.

First we consider that half of the particles carry a charge 10 times larger than the other half: $q_{\rm B} = 10q_{\rm A}$. The energy barriers for collisions between two A-particles, an A- and a B-particle, or two B-particles are now different:

$$E_{\rm AA} = \frac{q_{\rm A}^2}{d} < E_{\rm AB} = \frac{q_{\rm A}q_{\rm B}}{d} < E_{\rm BB} = \frac{q_{\rm B}^2}{d}\ . \tag{39}$$

As A-particles repell each other much less, one expects them to collide more frequently than B-particles. Remarkably the granular temperature of the A-particles and the B-particles remained the same in our simulations: A-particles that have lost part of their kinetic energy in a collision are stirred up by the strongly charged particles. The redistribution of kinetic and potential energy happens so quickly that the weakly and the strongly charged particles do not decouple thermally. This is in contrast to uncharged systems [46].

Based on the results for uniformly charged particles we postulate that the dissipation rate due to collisions between particles $\alpha$ and $\beta$ (A or B) is approximately given by

$$\gamma_{\alpha\beta} = \gamma_0 \cdot g_{\rm hs} \cdot p_{\alpha\beta} \cdot \exp\left(-\frac{E_{\alpha\beta}}{mT}\left(1-\frac{d}{\ell}\right)^2\right), \tag{40}$$

where $p_{\rm AA} = c_{\rm A}^2$, $p_{\rm AB} = 2c_{\rm A}c_{\rm B}$ and $p_{\rm BB} = c_{\rm B}^2$ with the concentration $c_{\rm A} = 1 - c_{\rm B}$ of A-particles (in our simulation $c_{\rm A} = c_{\rm B} = 1/2$). Fig.7 shows a comparison of (40) with simulation results for a two dimensional system with solid fraction $\nu = 0.09$ and coefficient of restitution $e_{\rm n} = 0.97$. The agreement for high granular temperatures is excellent. For low granular temperatures there are slight systematic deviations. These deviations are probably due to the fact that the Ansatz for the effective Coulomb barrier $E_{\alpha\beta}\left(1-\frac{d}{\ell}\right)^2$ in (40) is too naiv.

Now we apply (40) to compare the dissipation rates $\gamma = \gamma_{\rm AA} + \gamma_{\rm AB} + \gamma_{\rm BB}$ for systems with general bimodal charge distributions, where all charges have equal sign. Two independent parameters characterize the charge distribution for given total charge $N\bar{q}$ in the system with $N$ particles. These are the concentration $c_{\rm A}$ of the weakly charged particles and their charge, $q_{\rm A}$. The concentration and charge of the strongly charged particles are given by

$$c_{\rm B} = 1 - c_{\rm A}, \quad q_{\rm B} = \frac{\bar{q} - c_{\rm A}q_{\rm A}}{c_{\rm B}}. \tag{41}$$

As the physics does not depend on the sign of the charges, as long as it is the same for all particles, we may assume in the following that $0 \le q_{\rm A} \le \bar{q}$. The concentration parameter is restricted to the interval $0 \le c_{\rm A} < 1$.

We now show, that

$$\frac{\partial\gamma(c_{\rm A}, q_{\rm A})}{\partial c_{\rm A}} \ge 0 \tag{42}$$

and

$$\frac{\partial\gamma(c_{\rm A}, q_{\rm A})}{\partial q_{\rm A}} \le 0\,. \tag{43}$$

Since uniformly charged systems correspond to the lower boundary of the concentration interval, $c_{\rm A} = 0$, or the upper boundary of the charge interval, $q_{\rm A} = \bar{q}$, repectively, (42) and (43) imply that for a given average charge $\bar{q}$ the lowest collision rate (or dissipation rate) is reached, if all particles carry the same charge, $barq$.

In order to prove the inequalities (42) and (43) it is convenient to introduce the normalized quantities

$$\tilde{\gamma}_{\alpha\beta} = \gamma_{\alpha\beta}/\gamma_0 g_{\rm hs} \quad , \qquad \tilde{q}_\alpha = (q_\alpha/\sqrt{dmT})(1 - d/\ell) \tag{44}$$

so that $\tilde{\gamma}_{\alpha\beta} = p_{\alpha\beta}\exp(-\tilde{q}_\alpha\tilde{q}_\beta)$. Using (41) one obtains

$$\frac{\partial\tilde{\gamma}}{\partial c_{\rm A}} = 2c_{\rm A}e^{-\tilde{q}_{\rm A}^2} + 2\left(c_{\rm B} - c_{\rm A} - c_{\rm A}c_{\rm B}\tilde{q}_{\rm A}\frac{\partial\tilde{q}_{\rm B}}{\partial c_{\rm A}}\right)e^{-\tilde{q}_{\rm A}\tilde{q}_{\rm B}} - 2c_{\rm B}\left(1 + c_{\rm B}\tilde{q}_{\rm B}\frac{\partial\tilde{q}_{\rm B}}{\partial c_{\rm A}}\right)e^{-\tilde{q}_{\rm B}^2}. \tag{45}$$

Inserting $\partial\tilde{q}_{\rm B}/\partial c_{\rm A} = (\tilde{q}_{\rm B} - \tilde{q}_{\rm A})/c_{\rm B}$ this can be written in the form

$$\frac{e^{\tilde{q}_{\rm A}^2}}{2c_{\rm A}}\frac{\partial\tilde{\gamma}}{\partial c_{\rm A}} = \left[1 - (1 + \tilde{q}_{\rm A}(\tilde{q}_{\rm B} - \tilde{q}_{\rm A}))\,e^{-\tilde{q}_{\rm A}(\tilde{q}_{\rm B} - \tilde{q}_{\rm A})}\right]$$

$$+\frac{c_{\rm B}}{c_{\rm A}}e^{-\tilde{q}_{\rm A}(\tilde{q}_{\rm B} - \tilde{q}_{\rm A})}\left[1 - (1 + \tilde{q}_{\rm B}(\tilde{q}_{\rm B} - \tilde{q}_{\rm A}))\,e^{-\tilde{q}_{\rm B}(\tilde{q}_{\rm B} - \tilde{q}_{\rm A})}\right]. \tag{46}$$

As $1 + \tilde{q}_\alpha(\tilde{q}_{\rm B} - \tilde{q}_{\rm A}) \le \exp(\tilde{q}_\alpha(\tilde{q}_{\rm B} - \tilde{q}_{\rm A}))$ , both square brackets and hence the whole expression (46) are non-negative, as asserted in (42).

Similarly one calculates

$$\frac{\partial\tilde{\gamma}}{\partial\tilde{q}_{\rm A}} = -2c_{\rm A}^2\tilde{q}_{\rm A}e^{-\tilde{q}_{\rm A}^2} - 2c_{\rm A}c_{\rm B}(\tilde{q}_{\rm B} + \tilde{q}_{\rm A}\frac{\partial\tilde{q}_{\rm B}}{\partial\tilde{q}_{\rm A}})e^{-\tilde{q}_{\rm A}\tilde{q}_{\rm B}} - 2c_{\rm B}^2\tilde{q}_{\rm B}\frac{\partial\tilde{q}_{\rm B}}{\partial\tilde{q}_{\rm A}}e^{-\tilde{q}_{\rm B}^2}. \tag{47}$$

Using $\partial\tilde{q}_{\rm B}/\partial\tilde{q}_{\rm A} = -c_{\rm A}/c_{\rm B}$ this becomes

$$-\frac{1}{2c_{\rm A}}\frac{\partial\tilde{\gamma}}{\partial\tilde{q}_{\rm A}} = c_{\rm A}\tilde{q}_{\rm A}\left(e^{-\tilde{q}_{\rm A}^2} - e^{-\tilde{q}_{\rm A}\tilde{q}_{\rm B}}\right) + c_{\rm B}\tilde{q}_{\rm B}\left(e^{-\tilde{q}_{\rm A}\tilde{q}_{\rm B}} - e^{-\tilde{q}_{\rm B}^2}\right) \tag{48}$$

As both terms on the right hand side are obviously positive this proves (43).

It is not difficult to prove along the same lines that

$$\gamma_{\mathrm{AB}} \leq \gamma_{\mathrm{AB}_1} + \gamma_{\mathrm{AB}_2}, \tag{49}$$

if one splits up the B-fraction according to $c_{\mathrm{B}} = c_{\mathrm{B}_1} + c_{\mathrm{B}_2}$ and $c_{\mathrm{B}} q_{\mathrm{B}} = c_{\mathrm{B}_1} q_{\mathrm{B}_1} + c_{\mathrm{B}_2} q_{\mathrm{B}_2}$. Moreover, the above result, that a uniform charge leads to a smaller collision rate than any bimodal distribution, implies also

$$\gamma_{\mathrm{BB}} \leq \gamma_{\mathrm{B}_1\mathrm{B}_1} + \gamma_{\mathrm{B}_1\mathrm{B}_2} + \gamma_{\mathrm{B}_2\mathrm{B}_2}\,. \tag{50}$$

Likewise, the A-fraction can be split up, and the whole procedure can be applied iteratively, so that we reach the conclusion that the collision rate for any charge distribution is higher than for the case, where all particles carry the average charge.

It should be noted, however, that a broader charge distribution with fixed average charge $\bar{q}$ does not necessarily lead to a larger collision rate. In order to show this, we return to the bimodal distribution as an example. The variance of the charge distribution is

$$\sigma^2(c_{\mathrm{A}}, q_{\mathrm{A}}) = c_{\mathrm{A}}(q_{\mathrm{A}} - \bar{q})^2 + c_{\mathrm{B}}(q_{\mathrm{B}} - \bar{q})^2 = \frac{c_{\mathrm{A}}}{1 - c_{\mathrm{A}}}(q_{\mathrm{A}} - \bar{q})^2\,. \tag{51}$$

The partial derivatives of $\gamma$, (42) and (43), have the same signs as the corresponding partial derivatives of $\sigma^2$:

$$\frac{\partial \sigma^2}{\partial c_{\mathrm{A}}} = \left(\frac{\bar{q} - q_{\mathrm{A}}}{1 - c_{\mathrm{A}}}\right)^2 \geq 0, \qquad \frac{\partial \sigma^2}{\partial q_{\mathrm{A}}} = -2c_{\mathrm{A}}\left(\frac{\bar{q} - q_{\mathrm{A}}}{1 - c_{\mathrm{A}}}\right) \leq 0\,. \tag{52}$$

However, as $\nabla\gamma = (\partial\gamma/\partial c_{\mathrm{A}}, \partial\gamma/\partial q_{\mathrm{A}})$ and $\nabla\sigma^2 = (\partial\sigma^2/\partial c_{\mathrm{A}}, \partial\sigma^2/\partial q_{\mathrm{A}})$ are not parallel, one can always find parameter changes $d\mathbf{p} = (dc_{\mathrm{A}}, dq_{\mathrm{A}})$ such that $d\gamma = \nabla\gamma \cdot d\mathbf{p}$ and $d\sigma^2 = \nabla\sigma^2 \cdot d\mathbf{p}$ have opposite signs.

## VII. DISCUSSION

We derived the dissipation rate of a charged granular gas, where all charges have the same sign. Compared to the uncharged case the dissipation rate is exponentially suppressed by a Boltzmann factor depending on the ratio between the Coulomb barrier and the granular temperature.

In the derivation we assumed a Gaußian velocity distribution, although it is known that in the uncharged case deviations from a Gaußian behaviour emerge due to the inelastic collisions [34]. These deviations, however, were shown to have little effect on the dissipation rate [35]. As the system becomes less dissipative in our case, it is reasonable to expect that the effect of deviations from a Gaußian velocity distribution will be even weaker.

In a dense system particle correlations enter the collision statistics and hence the dissipation rate in two ways: First there is the well known Enskog correction as in the uncharged case. It describes that the excluded volume of the other particles enhances the probability that two particles are in contact. Second the Coulomb barrier which colliding particles must overcome is reduced and will vanish in the limit of a dense packing.

These results were obtained for periodic boundary conditions, so that the system remained homogeneous. We showed, however, that it may be applied locally in the case, where walls induce inhomogeneous solid fraction and granular temperature. This inhomogeneity is opposite to the one induced by flow of uncharged grains through a vertical pipe. Therefore we could conclude that the Coulomb repulsion reduces the flow velocity.

Coulomb repulsion slows collisional cooling down from the $t^{-2}$-decay to a behaviour like $1/\ln t$, when $T(t)$ drops below $T_{\mathrm{c}} = E_{\mathrm{eff}}/m$, which means that the average kinetic energy of the grains does not suffice to overcome the Coulomb repulsion.

Finally we considered a bimodal charge distribution (both charges of equal sign), which leads to more frequent collisions among the weakly charged particles than among the strongly charged ones. Nevertheless the two kinds of particles kept the same granular temperature. We pointed out, how the dissipation rate for such a system can be evaluated. If the charge gets redistributed among the particles ($q_{\mathrm{A}} \to q_{\mathrm{A}} + \delta q$, $q_{\mathrm{B}} \to q_{\mathrm{B}} - (c_{\mathrm{A}}/c_{\mathrm{B}})\delta q$) for fixed concentrations, then the dissipation rate increases with the variance of the charge distribution. In particular the dissipation rate is minimal, if all particles have the same charge. More general we concluded that any deviation from uniform charging in a system with given total charge increases the collision rate.

An important question, which remained open in this paper, concerns the influence of charge transfer processes on the collision statistics. In the present investigation all particles retained their charges, even if there was a charge difference. Therefore our theory need to be modified for metallic particles.

**Acknowledgements**

We thank Lothar Brendel, Haye Hinrichsen, Zeno Farkas, Alexander C. Schindler and Hendrik Meyer for useful comments. We gratefully acknowledge support by the Deutsche Forschungsgemeinschaft through grants No. Wo 577/1-2 and Hi 744/2-1.

## APPENDIX A: COMPUTER SIMULATION METHOD

Distinct element (or molecular dynamics (MD)) simulations [17] are usually done with *time step driven* or *event driven* algorithms [36]. None of them is well suited for investigating a charged granular gas. Therefore we developed a new simulation scheme, which combines the virtues of both and will be described in this section.

We use a "brute force" MD algorithm, which is simple and sufficient for our problem. More sophisticated ways of dealing with the long range interactions, such as the multipolar expansion [37], the particle-particle-particle-mesh [38] or the hypersystolic algorithms [39] should be used, if larger systems need to be studied.

The event driven method for simulating the motion of all particles in the granular gas can be applied, whenever the particle trajectories between collisions can be calculated analytically, so that the time interval between one collision event and the next can be skipped in the simulation. Obviously this is impossible in a system with long range Coulomb interactions. However, the idea to avoid the detailed resolution of a collision event in time is still applicable. So the velocities of the collision partners are simply changed instantaneously to the new values predicted by momentum and angular momentum conservation and an energy loss determined by the restitution coefficient. We shall keep this feature of event driven simulations.

In the time step driven simulation method the equations of motion of all particles in the granular gas are discretized using a fixed time step, which is small compared to the duration of a collision. Hence each collision, which is modeled as an overlap between particles, is temporally resolved in detail. This has the advantage, that the formation of long lasting contacts between particles can in principle be simultated realistically. If the particles carry equal charges, however, this will not happen, so that the collisions may be approximated as being instantaneous like in event driven simulations. Apart from being more efficient, this automatically avoids the so called brake-failure artifact [16], which hampers time-step driven molecular dynamics simulations with rapid relative motion. On the other hand, we need a time discretization of the particle trajectories between collisions, in order to take the changing electrostatic interactions properly into account.

Because of the long-range nature of the Coulomb potential, we have to include the interactions with the periodic images of the particles in the basic cell. One way to do this is by Ewald summation. Details of this method can be found in [17]. Another method is the *minimum image* convention: Only the nearest periodic image is taken into account for the calculation of the interactions. The minimum image method has the advantage, that it is much faster than the Ewald summation. We checked the validity of the minimum image method by comparison with the Ewald summation and found, that as long as $E_q/mT < 10$ both methods yield indistinguishable results. This upper limit for the coupling has been found before in Monte-Carlo simulations of the OCP [29]. As our systems all satisfy this condition, we used the minimum image convention.

[1] S. Kanazawa, T. Ohkubo, Y. Nomoto, T. Adachi; J. of Electrost. **35**, 47 (1995).
[2] S. Nieh, T. Nguyen; J. of Electrostatics **21**, 99 (1988).
[3] Sampuran Singh, G.L. Hearn; J. of Electrostatics **16**, 353 (1985).
[4] I.I. Inculet, G.S.P. Castle; Inst. Phys. Conf. Series, No. 188: Section 4, page 217; IOP Publishing Ltd (1991). A. Singewald, G. Fricke; Chem.-Ing.-Tech. **55**, 39 (1983).
[5] P.K. Haff; J. Fluid Mech. **134**, 401 (1983).
[6] F. Spahn, O. Petzschmann, K.-U. Thiessenhusen, J. Schmidt; in: Physics of Dry Granular Media, eds. H.J. Herrmann, J.-P. Hovi and S. Luding (Kluwer Acad. Publ., Dordrecht, 1998) pp. 401-406.
[7] F. Melo, P. Umbanhowar, H.L. Swinney; Phys. Rev. Lett. **72**, 172 (1993); **75**, 3838 (1995).
[8] T. Shinbrot, F. J. Muzzio; Nature **410**, 251 (2001).
[9] J. Eggers; Phys. Rev. Lett. **83**, 5322 (1999). D. van der Meer, K. van der Weele, D. Lohse; Phys. Rev. E **63**, 061304 (2001).
[10] I. Goldhirsch, G. Zanetti; Phys. Rev. Lett. **70**, 1619 (1993).
[11] S. McNamara, W.R. Young; Phys. Fluids A **4**, 496 (1992); Phys. Rev. E **53**, 5089 (1996).
[12] S. Luding; T.A.S.K. Quaterly, Scientific Bulletin of Academic Computer Centre of the Technical University of Gdansk, 2(3):417-443, July, 1998.
[13] S. Luding, H.J. Herrmann; 1999 preprint.

[14] J. Lowell, A.C. Rose-Innes; Adv. Phys. **29**, 947 (1980).
[15] M. Baus, J.P. Hansen; Phys. Rep. **59**, 1 (1980).
[16] J. Schäfer, D.E. Wolf; Phys. Rev. E **51**, 6154 (1995).
[17] M.P. Allen, D.J. Tildesley: *Computer Simulation of Liquids*; Clarendon Press, Oxford 1987.
[18] J. Schäfer, S. Dippel, D.E. Wolf; J. Phys. I (France) **6**, 5 (1996).
[19] N.V. Brilliantov, F. Spahn, J.-M. Hertzsch, T. Pöschel; Phys. Rev. E **53**, 5382 (1996).
[20] T. Koga; *Introduction to kinetic theory,* Pergamon Press, Oxford 1970.
[21] R.D. Present: *Kinetic Theory of Gases*; McGraw-Hill, New York 1958.
[22] C.K.L. Lun, S.B. Savage, D.J. Jeffrey, N. Chepurniy; J. Fluid Mech. **140**, 223 (1984).
[23] J.T. Jenkins, M.W. Richman; Archive for Rational Mechanics and Analysis **87**, 355 (1985).
[24] N.F. Carnahan, K.E. Starling; J. Chem. Phys. **51**, 635 (1969).
[25] R.G. Palmer, J.D. Weeks; J. Chem. Phys. **58**, 4171 (1973).
[26] J.P. Hansen, J.J. Weis; Mol. Phys. **5**, 1379 (1977).
J.P. Rino, O. Hipólito; Phys. Rev. E **48**, 1375 (1993).
H.S. Kang, F.H. Ree; J. Chem. Phys. **103**, 9370 (1995).
[27] E.E. Salpeter, H.M. Van Horn; Astrophys. J. **155**, 183 (1969).
[28] H.E. DeWitt, H.C. Graboske, M.S. Cooper; Astrophys. J. **181**, 439 (1973).
[29] S.G. Brush, H.L. Sahlin, E. Teller; J. Chem. Phys. **45**, 2102 (1966).
[30] N. Itoh, S. Ichimaru; Phys. Rev A **16**, 2178 (1977).
[31] Y. Rosenfeld; Phys. Rev. A **46**, 1059 (1992).
[32] H.E. DeWitt, H.C. Graboske, M.S. Cooper; Astrophys. J. **181**, 439 (1973).
[33] W.L. Slattery, G.D. Doolen, H.E. De Witt; Phys. Rev. A **21**, 2087 (1980); **26**, 2255 (1982).
[34] S.E. Esipov, T. Pöschel; J. Stat. Phys. **86**, 1385 (1997).
[35] T.P.C. van Noije, M.H. Ernst; Granular Matter **1**, 57 (1998).
[36] D. E. Wolf "Modelling and Computer Simulation of Granular Media", in: Computational Physics, eds. K. H. Hoffmann and M. Schreiber (Springer, Heidelberg, 1996) pp. 64-94
[37] A.J.C. Ladd; Mol. Phys. **33**, 1039 (1977); **36**, 463 (1978).
[38] J.W. Eastwood, R.W. Hockney, D. Lawrence; Comput. Phys. Commun. **19**, 215 (1980).
[39] T. Lippert, A. Seyfried, A. Bode, K. Schilling; IEEE Transactions on Parallel & Distributed Systems, vol.9, no.2, Feb. 1998, pp.97-108.
[40] I. Goldhirsch in: *Physics of Dry Granular Media,* eds H.J. Hermann, J.-P. Hovi and S. Luding; NATO ASI Series, Kluwer. NL-Dordrecht 1998.
[41] J.T. Jenkins, M.W. Richman; Phys. Fluids **28**, 3485 (1985).
[42] D. Henderson; Mol. Phys. **30**, 971 (1975).
[43] D.E.Wolf, T. Scheffler, J. Schäfer; Physica A **274**, 171 (1999).
[44] J. Schäfer: *Rohrfluss granularer Materie: Theorie und Simulation*, Doctoral Thesis, Gerhard-Mercator-Universität Duisburg, 1996.
[45] J.-L. Aider, N. Sommier, T. Raafat, J.-P. Hulin; Phys. Rev. E **59**, 778 (1999).
[46] A. Barrat, E. Trizac; Granular Matter **4**, 57 (2002).
[47] T. Scheffler, D.E. Wolf, in: *Molecular Dynamics on Parallel Computers*, eds. R. Esser, P. Grassberger, J. Grotendorst, M. Lewerenz (World Scientific, Singapore, 2000) pp. 233 – 238.
[48] T. Scheffler, D.E. Wolf, in: *Structure and Dynamics of Heterogeneous Systems*, eds. P. Entel, D.E. Wolf (World Scientific, Singapore, 2000) pp.131 – 139.
[49] The potential energy summed over all periodic images diverges.

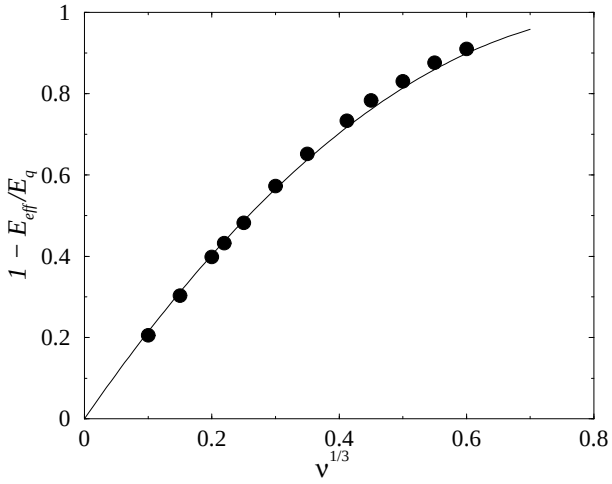


FIG. 2: The dependence of the effective energy barrier on the solid fraction. Filled circles correspond to computer simulations, the solid line is Eq. (24).

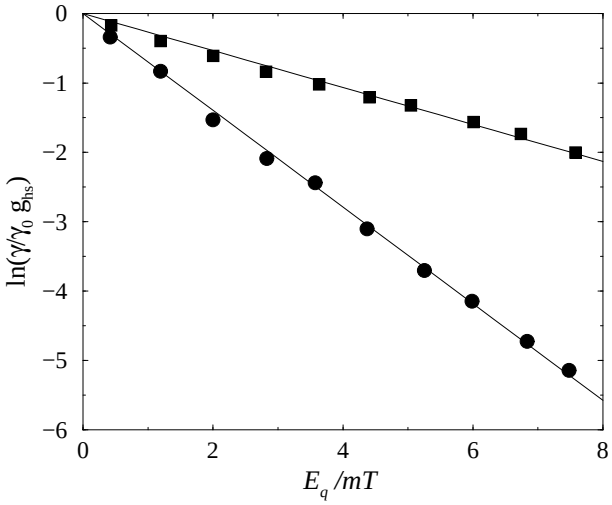


FIG. 1: Arrhenius-plot of the dissipation rate $\gamma$ normalised by the one of the uncharged system, Eq. (16). Granular temperature is scaled by $E_{\rm q}/m$. Filled circles correspond to simulations of density $\nu = 3.375 \cdot 10^{-3}$ and filled squares $\nu = 7 \cdot 10^{-2}$. The linear fits yield: $E_{\rm eff}/E_{\rm q} = 0.70$ for the lower density and $E_{\rm eff}/E_{\rm q} = 0.27$ in the other case.

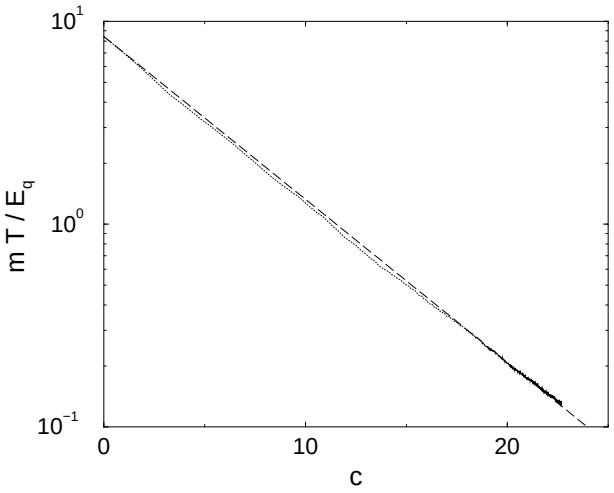


FIG. 3: Cooling of a sytem with density $\nu = 3.375 \cdot 10^{-3}$ and $e_n = 0.85$. The temperature is normalised by $E_q/m$ and $c$ is the number of collisions per particle. The dashed line is given by (31).

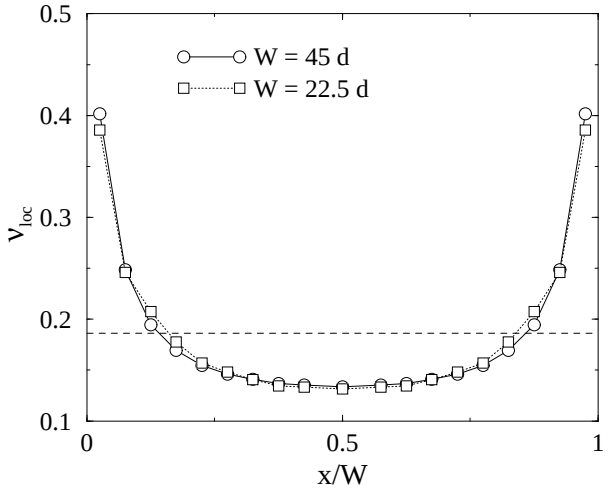


FIG. 4: Solid fraction of a charged granular gas in a two dimensional box with confining walls perpendicular to the $x$-direction and periodic boundary conditions in the $y$-direction. The dimensions of the box are $W \times L$ with $L = 60d$ and two different values of $W$. Because of Coulomb repulsion the particle concentration increases towards the wall. Because of the absence of screening the solid fraction profile depends approximately only on the scaled variable $x/W$, with small deviations due to the excluded volume interaction.

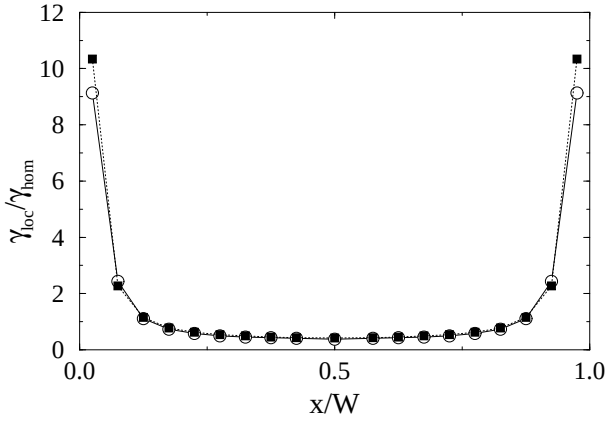


FIG. 5: Same system as Fig.4 with $W = 45d$. Open circles are the local dissipation rates, in units of the dissipation rate in a homogeneous system with solid fraction $\nu = 0.186$ at the average granular temperature in the box, $E_q/mT = 1.7$. The black squares are the dissipation rates calculated from (25) with the local solid fraction (see Fig.4) and the local granular temperature.

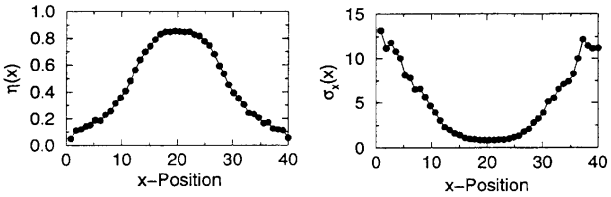


FIG. 6: Local solid fraction $\eta$ (left) and root mean square fluctuation of the horizontal velocity component (right) for granular flow through a two dimensional vertical pipe. The quantities are averaged over layers parallel to the wall in order to show their $x$-dependence. The diameter of the pipe is 40 $d$. From [44].

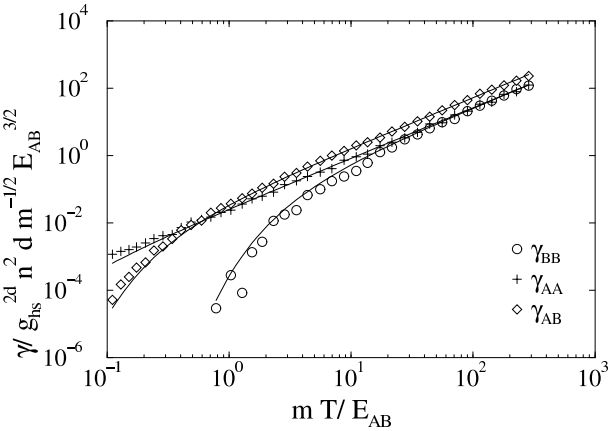


FIG. 7: Dissipation rates $\gamma_{\alpha\beta}$ as a function of granular temperature in convenient units. There are equal numbers of particles A and B in the system, which differ only by their charges, $q_A = 0.1q_B$. At high granular temperatures the dissipation rates due to A-A, B-B, or A-B collisions, respectively, obey a $T^{3/2}$ power law, where $\gamma_{AB}$ is larger by a factor of 2 compared to the other two curves, because $p_{AA} = p_{BB} = p_{AB}/2$. For decreasing $T$ first the collisions between the strongly charged B-particles are suppressed. For $E_{AA}/E_{AB} \ll mT/E_{AB} \ll 1$ only collisions between A-particles still contribute to the dissipation rate. For still smaller granular temperature (not shown) also this contribution will be suppressed. The curves are given by the theoretical formula (40).